Triplet Fusion Upconversion for Photocuring 3D Printed Particle-Reinforced Composite Networks

Jitkanya Wong†, Shixuan Wei†, Rinat Meir, Naroa Sadaba, Nathan A. Ballinger, Elizabeth K. Harmon, Xin Gao, Gokce Altin-Yavuzarslan, Lilo D. Pozzo, Luis M. Campos, Alshakim Nelson**

J. Wong, N. Sadaba, N. A. Ballinger, G. Altin-Yavuzarslan, A. Nelson
Department of Chemistry, University of Washington, Seattle, WA 98195, USA
E-mail: alshakim@uw.edu

S. Wei, R. Meir, X. Gao, L. M. Campos
Department of Chemistry, Columbia University, New York, NY 10027, USA
E-mail: lcampos@columbia.edu

N. Sadaba
POLYMAT and Department of Polymers and Advanced Materials: Physics, Chemistry and Technology, Faculty of Chemistry, University of the Basque Country UPV/EHU, Donostia-San Sebastián 20018, Spain

E. K. Harmon, L. D. Pozzo
Department of Chemical Engineering, University of Washington, Seattle, WA 98195, USA

Keywords: 3D Printing, Direct-ink-write Printing, Triplet-Triplet Annihilation Upconversion, Photopolymerization, Hydrogels, Composites

High energy photons (λ<400 nm) are frequently used to initiate free radical polymerizations to form polymer networks, but are only effective for transparent objects. This phenomenon poses a major challenge to additive manufacturing of particle-reinforced composite networks since deep light penetration of short-wavelength photons limits the homogeneous modification of physicochemical and mechanical properties. Herein, we employ the unconventional, yet versatile multiexciton process of triplet-triplet annihilation upconversion (TTA-UC) for curing opaque hydrogel composites created by direct-ink-write (DIW) 3D printing. TTA-UC converts low-energy red light (λ_{max} = 660 nm) for deep penetration into higher-energy blue light to

initiate free radical polymerizations within opaque objects. As proof-of-principle, hydrogels containing up to 15 wt% TiO_2 filler particles and doped with TTA-UC chromophores were readily cured with red light, while composites without the chromophores and TiO_2 loadings as little as 1-2 wt% remained uncured. Importantly, this method has wide potential to modify the chemical and mechanical properties of complex DIW 3D printed composite polymer networks.

Additive manufacturing (AM or 3D printing) involves selective deposition of materials in a layer-by-layer fashion to create customizable structures with precise 3-dimensional control. As AM evolves from a rapid prototyping process to a key driver toward the next industrial revolution, significant progress has been made towards developing advanced printable materials.[1–6] In many AM techniques, printing robust 3D objects relies on the formation of polymer networks via photoinitiated radical polymerizations to achieve the desired mechanical properties.[7,8] Photopolymerization is a preferred method as it is fast and can be done at ambient temperature with spatiotemporal control. Network formation can occur during the printing process, in which patterned light is used to generate the 3D object.[9,10] Alternatively, network formation can be photoinitiated in a post-print cure step that occurs after the printing process is complete.[11,12] Both of these processes commonly use high energy light with wavelengths below ≤405 nm to generate radicals that initiate polymerization.[13–15] However, light penetration depth becomes increasingly critical in the fabrication of objects with homogeneous physicochemical and mechanical properties as the thickness of the printed part exceeds millimeter length scales. The penetration depth of light with short wavelength (such as UV) is limited due to the absorption and scattering in most materials (including biological tissues).[16,17] Hence, photopolymerization with high energy light can require a longer exposure time or higher intensity, which increases energy consumption, risks dehydration of the hydrogels, and causes issues related to degradation.[18] While homogenous curing of thick and/or visually opaque materials to create uniform polymer networks would be beneficial for applications in particle

composites or tissue engineering, this capability remains a significant challenge for the AM field.

Triplet-triplet annihilation upconversion (TTA-UC) is a process that effectively converts low energy photons[19] (long wavelength) into high-energy excitons, which can then emit short-wavelength irradiation or undergo energy transfer processes. Thus, we reason that this mechanism could present a facile methodology to cure polymer networks using conventional long-wavelength irradiation sources, devoid of highly specialized photochemical equipment. For example, two-photon polymerization (TPP) takes advantage of the deep penetration of red and infrared light to fabricate 3D objects.[20–24] However, the necessity for a single molecule to simultaneously absorb two photons requires an expensive laser set-up with high fluences. Similarly, Zhu, et al. demonstrated an application of DIW printing of pigmented inks using NIR-driven upconversion with inorganic nanoparticles.[25] Although upconversion using inorganic nanoparticles can also initiate photopolymerization with low energy photons[26], this technique requires a high excitation power density due to a lower absorption of visible excitation light and quantum yield of the materials.[19] Alternatively, TTA-UC involves two chromophores[27], a sensitizer and an annihilator, and benefits from the high extinction coefficient of the sensitizers to achieve excitation at a relatively low light fluence.[28] The ability to employ TTA-UC to initiate polymerizations is rapidly gaining traction due to the versatility of the systems used, especially in molding and printing 3D polymeric objects.[29,30] Considering the vast advantages resulting from doping plastics with fillers to reinforce and alter mechanical properties of thermoplastics and thermosets, it is imperative to develop photochemistries that yield reinforced composites by light irradiation in order to access chemically tunable 3D printed objects made from materials that are sensitive to thermally-driven molding processes.

Herein, we introduce a modular strategy for multimaterial direct-ink-write (DIW) 3D printing composites and subsequent light-curing of thick and optically opaque hydrogels mediated by TTA-UC. We utilized a benchtop red light source (660 nm) to cure combinations

of transparent hydrogels and opaque TiO_2 reinforced hydrogels. In order to test how TTA-UC compares to conventional UV light photocuring post-3D printing, core-shell objects were fabricated with a hydrogel core and TiO_2-reinforced hydrogel shell. The limited penetration of UV light through the composite layer resulted in a "jammy gel" composite, comprising a cured shell and uncured core (**Figure 1**A). In contrast, the construct cured via TTA-UC was cured through its entirety to afford a "hard-cured gel." These results highlight the remarkable potential of implementing TTA-UC to facilitate photoinitiated polymer network formation through thick and opaque 3D printed objects that cannot be uniformly cured otherwise.

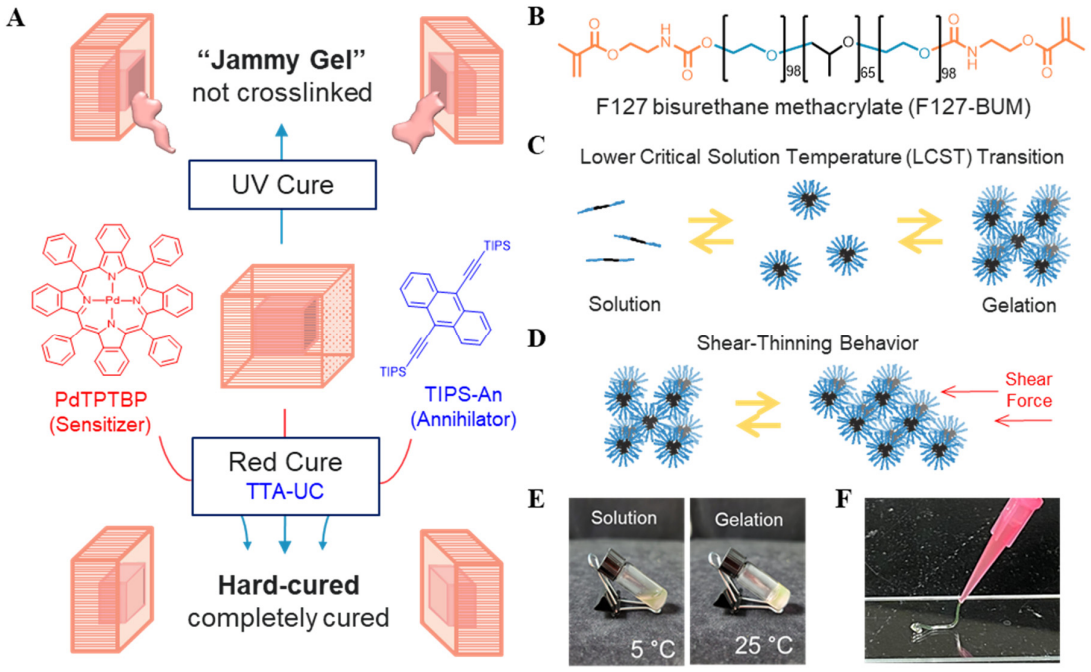

Figure 1. Design and formulation of TTA-UC hydrogel system. A) Our strategy was to cure a hydrogel composite with an opaque component by using low energy red light, which offered better penetration into most opaque materials and exploited the TTA-UC to obtain blue light to initiate crosslinking. B) Our selected base material, F127-BUM hydrogel, forms micelles when dissolved in water and can undergo LCST transition (C) and shear-thinning behavior (D). Upon addition of the TTA-UC system, the hydrogel retains its ability to undergo LCST sol-gel transition (E), and shear thin (F).

For this study, we used F127 bisurethane methacrylate (F127-BUM), which is a triblock copolymer that forms a versatile temperature responsive and shear-thinning hydrogel

ink for DIW 3D printing (**Figure 1**B).[31] The hydrogel undergoes a temperature dependent sol-gel transition at ~17 °C[32,33], which enables additives to be incorporated homogeneously while in its liquid form at low temperatures (5 °C). Upon warming to ambient temperature, the material becomes a self-supporting and shear-thinning gel that can be extruded from a nozzle to fabricate 3D constructs. Typically, a photoradical generator such as 2-hydroxy-4'-(2-hydroxyethoxy)-2-methylpropiophenone[34] (Irgacure 2959) or Eosin Y/triethanolamine[35] is included in the crosslinkable F127 gel formulation for photocuring the construct. Thus, a hydrogel comprising a continuous polymer network can be formed by UV photoinitiated free radical polymerization of the F127-BUM chain ends with Irgacure 2959.

To overcome the limitations of UV photoinitiated systems for hydrogels that absorb or scatter UV light, F127-BUM hydrogels were formulated with TTA-UC chromophores that could be incorporated within aqueous media.[36] Matching the absorption profile of Eosin Y was accomplished using the combination of palladium(II) meso-tetraphenyl tetrabenzoporphyrin (PdTPTBP) and 9,10-bis((triisopropylsilyl)ethynyl)anthracene (TIPS-anthracene), a sensitizer and annihilator, respectively (**Figure 1**A, and **Figure S2**, Supporting Information).[37] The TTA-UC chromophores were dissolved in a mixture of tetrahydrofuran (THF) and soybean oil, the latter acting as an oxygen scavenger necessary to avoid quenching of triplet excitons.[38] A conventional photoredox initiator system based on Eosin Y and triethanolamine (TEA) was chosen since it can be activated using blue light emitted by TIPS-anthracene (**Figure S2**, Supporting Information).[39,40] The TTA-UC system is introduced to the 30 wt% F127-BUM hydrogel via addition of the sensitizer + annihilator, Eosin Y, and TEA solutions, followed by vortexing. While incorporation of other additives into hydrogels can change the polymer-polymer and polymer-solvent interaction gelation[41–44], our hydrogel with the TTA-UC system did not exhibit a significant shift in LCST (**Figure 1**C, E) and retains shear thinning behavior (**Figure 1**D, F). F127-BUM self-assembles in aqueous media to form micelles that pack into ordered lattices that give rise to the gel state.[45] Characterization of these

hydrogels by SAXS confirmed that the addition of the upconversion components did not disrupt the assembled structure of micelles with ordered BCC packing, consistent with another study that observed BCC packing in purified F127.[46] The viscoelastic properties of the hydrogel inks were characterized by rheometric experiments that suggest the addition of the TTA-UC components to the F127-BUM hydrogel does not affect its viscoelastic behaviors required for extrusion-based 3D printing (**Figure S5**, **S6**, Supporting Information).

To verify the effect of upconversion in the photocuring, the F127-BUM hydrogel containing TTA-UC additives was photocured with red (660 nm), and compared to a control hydrogel (containing sensitizer, initiator system, but no annihilator, i.e. TIPS-anthracene). As shown in **Figure S3**A, only the TTA-UC hydrogel crosslinked under red light. This result demonstrates that without the annihilator, the photoinitiator system remains inactive when exposed to red light, and no crosslinking was observed. We further confirmed the crosslinking using a frequency sweep rheometric experiment on the hydrogel pre- and post-cured with red light. The storage modulus increased three-fold after crosslinking and was stable across a range of frequencies over time, suggesting irreversible crosslinking (**Figure S3**B, Supporting Information).

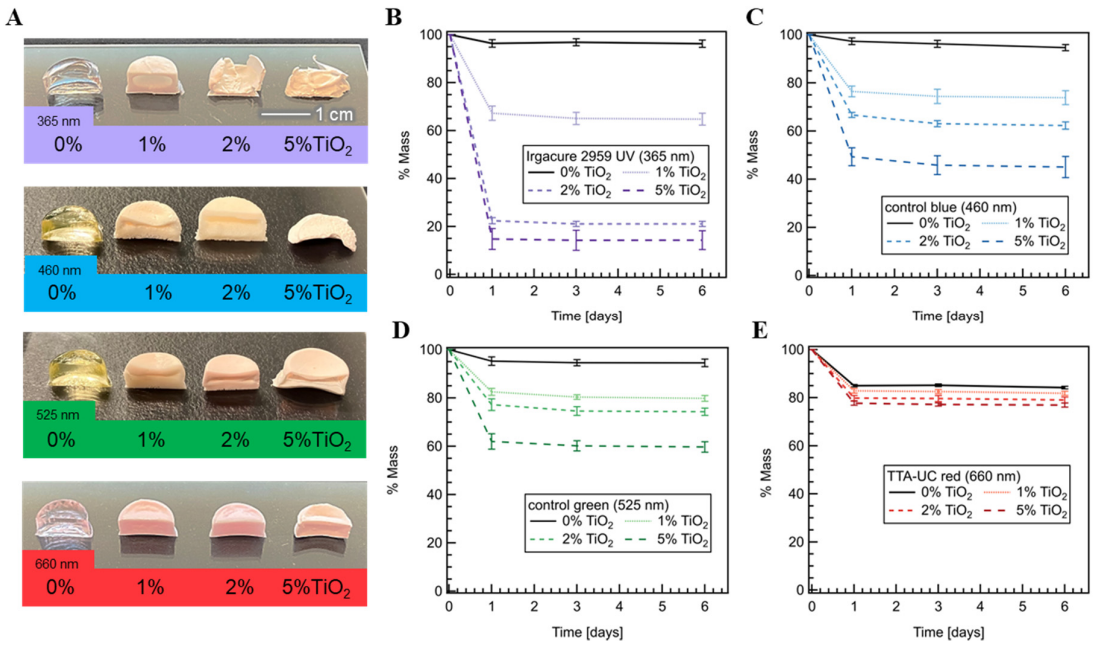

Figure 2. Hydrogels cured with different wavelengths. A) Cross-sections of samples with increasing amounts of TiO_2 (325 mesh) cured under 365 nm (traditional UV curing with Irgacure 2959), 460 nm, 525 nm, (direct excitation of Eosin Y), and 660 nm (TTA-UC) light, after 6 days of acetone extraction, dehydrated and reswollen with deionized water. Tracked mass loss during gel fraction experiments for samples cured using UV (B), blue (C), green (D), and red light (E). The transparent samples (0 wt% TiO_2) have a higher extent of curing when irradiated with UV light, but curing was sluggish when TiO_2 was added. Gel fraction of samples containing TiO_2 were less impacted, especially with long-wavelength irradiation.

Inorganic fillers have been added to hydrogels to reinforce and modify the mechanical properties[47,48], but have limited function in photocurable materials as addition of the fillers reduces the transparency of the matrix.[49] As a representative example, we included TiO_2 (325 mesh, **Figure S10** and **Figure S11**, Supporting Information) particles in our hydrogels, which allowed us to test whether using red light can offer an advantage in deeper light penetration through opaque materials. In order to demonstrate this, we added varying amounts of TiO_2 particles into the hydrogel to reduce the transparency of the material. The gels were cast into a mold, cured, then cut in half to observe the extent of curing inside. To compare the effect of light irradiation with different wavelengths on curing, three hydrogel systems with TiO_2 particles were studied: an Irgacure 2959 hydrogel (**Table S2**, cured by UV), Eosin Y/TEA hydrogel (**Table S3**, cured by blue or green light), and TTA-UC hydrogel (**Table S1**, cured by red light). While samples cured with UV, blue or green light have uncured material in the center (more with increasing wt% of TiO_2 particles), all samples cured with red light were entirely crosslinked through the center (**Figure 2**A). This observation was further quantified through gel fraction experiments, where the samples were cut in half and any material not crosslinked into the network was extracted with acetone. For transparent samples without TiO_2, the gel fraction for samples cured using UV light retained 96.2±1.5 wt% of the original polymer mass, but the samples cured using red light retained 84.21±0.55 wt%. We posit that potential side-reactions with the alkene groups in soybean oil could decrease the gel-fraction[50], which may be circumvented using other oxygen scavengers. On one hand, as we increased the amount of TiO_2, the mass fractions of samples cured with 365 nm light (**Figure 2**B) rapidly decreased,

going from 64.7±2.5% (1 wt% TiO_2), to 21.1±1.1% (2 wt% TiO_2), to 14.3±3.9% (5 wt% TiO_2). Similar trends were observed for TiO_2 hydrogels with direct excitation of Eosin Y/TEA using blue and green light irradiation. Additionally, we observed higher gel fractions as the irradiation wavelength increased (**Figure 2**C, D). On the other hand, the mass fractions for samples cured with 660 nm light (**Figure 2**E) were very close to each other, between 81.83±0.87%(1 wt% TiO_2) and 76.91±0.96% (5 wt% TiO_2). The similar mass fractions suggested that samples cured using red light were not affected by addition of particles that reduce transparency, allowing the hydrogels to cure consistently throughout the structure. Through the same rheometric frequency sweep experiments as **Figure S3**B, we demonstrated successful red light curing for hydrogels containing up to 15 wt% TiO_2 (**Figure S7**, Supporting Information). The differences in mechanical properties of the hydrogel composites were determined in uniaxial tensile experiments on dogbones that were cast and cured using red light, shown in **Figure 3** and summarized in **Table S4**. In general, the hydrogels became stiffer with increasing amounts of TiO_2 particles.

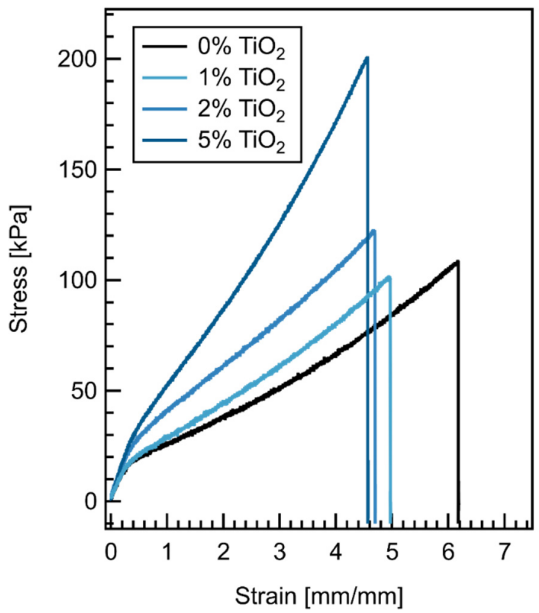

Figure 3. Tensile stress-strain curves for hydrogel dogbone (ASTM D638 type V) samples with varying amounts of TiO_2 (325 mesh), cured by TTA-UC with 660 nm light.

DIW printing enables the fabrication of multi-material objects without the need for a highly customized printer such as multi-wavelength printer[10,51], and the ability to print with compositional variations throughout the printed structure.[52–55] This form of AM also allows us to print the entire structure before photocuring, which enables polymer networks to be formed in the x, y, and z directions, and across the extruded filament boundaries. As a result, interlayer defects and interfacial boundaries between contrasting materials of a multi-material print were minimized, resulting in improved mechanical properties.[56,57] Therefore, multi-material DIW 3DP of hydrogel composites can be used to simulate biological systems comprising a complex scaffold of multiple cell type domains with varying mechanical properties.[58–60] As shown in **Figure 4**, various architectures of dual composite materials of gels with and without particle additives were printed using a HyRel mechanical extrusion printer. The hydrogel and composite inks were readily transferred into syringes for extrusion while in their sol state at ~5 °C. The inks were extruded through a 20-gauge nozzle (0.603 mm I.D.) to produce filaments with 0.67 mm diameter to fabricate multi-material objects that could vary in their composition in the x, y, and z directions (**Figure 4**A, B). First, we printed a clear hydrogel layer sandwiched between 2 opaque hydrogel layers (**Figure 4**C), followed by irradiation with the light source above the opaque layer. Using traditional UV curing with Irgacure 2959 clearly resulted in a sluggishly cured gel that lost its shape when pressed. On the other hand, implementing TTA-UC to mediate photocuring resulted a thoroughly cured, mechanically robust polymer network. Another key advantage of the polymers used is that the interface between the opaque and clear layers contains methacrylic groups that can effectively fuse the entire construct. Thus, the multi-material print maintained its spatially and compositionally defined regions even after cutting through the object.

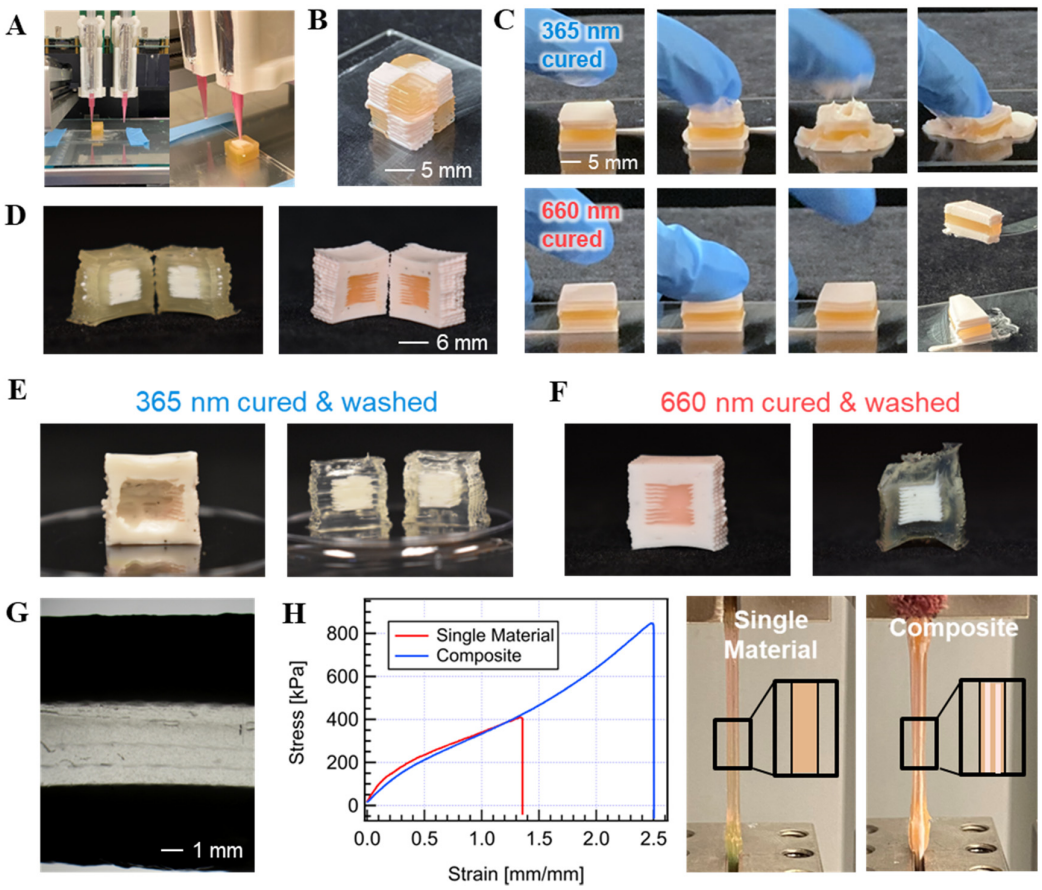

Figure 4. Multi-material DIW 3DP demonstrations using a HyRel extrusion printer (A). Prints include with changing materials in x,y,z directions B) checkered cube, C) sandwich cured under both UV and red light, where the UV cured structure was not cured entirely, and D) core-shell structure. The structures in (D) are cured and washed and shown in (E) and (F). E) The UV cured structure on the right side is not cured completely, but F) red light cured structures were both completely cured. G) Optical microscopy image of sandwich (1 mm slice) in (C). H) Tensile test for printed single material (0% TiO_2) and composite (alt. layers 0/1% 325 mesh TiO_2) dogbones; the insets are graphical representations for clarity (EN ISO 527-2:1996 type 5B).

To challenge the photocuring process mediated by TTA-UC in opaque constructs, we devised an experiment to test the chemistry of core-shell objects (**Figure 4**D). The printed constructs were cured with UV or red light, and then submerged in water to remove the uncured material. To our surprise, the cube structures with a transparent shell cured entirely under both conditions. Although UV light cannot penetrate through opaque regions, it is possible for the radical polymerization that initiates in the transparent regions to then propagate into the opaque section. However, the structure with the opaque shell led to drastic differences when irradiated

with UV vs. red light. While the entire structure can be cured throughout by red light, the same structure irradiated with UV light exhibited a significant amount of uncured material in both layers, as evidenced by the presence of a void in the center of the cube (**Figure 4**E, F). Although transparent, the core of the structure was not cured when using UV light.

Lastly, we explored the opportunity to exploit DIW printing of composites to create complex structures with mechanical reinforcement furnished by particle additives. Prior studies of gels with gradient layered structures highlight the importance of varying the mechanical properties within molded objects.[61] Thus, we printed composites with macroscopically well-defined interfaces between particle-reinforced and pristine gels. An optical microscopy image of a cross section (**Figure 4**G) of the structure from **Figure 4**C left in water for 1 month showed distinct separation between the materials (dark area = 1% 325 mesh TiO_2, transparent area = 0% TiO_2), revealing precise spatial control of printed materials by DIW. To compare differences in the mechanical properties of pristine and composite structures, we printed pristine gels and layered composite dogbones (five alternating layers of transparent hydrogel and TiO_2 hydrogel composite). Uniaxial tensile experiments revealed that composite dogbones can undergo twice the stretching distance before failure, suggesting a potential to use TiO_2/hydrogel composite as reinforcement layers to the overall printed structure (**Figure 4**H). Interestingly, the Young's modulus of both systems remains the same. These results underscore the importance of photocurable-particle reinforced 3D printed objects.

In summary, we demonstrated how an unconventional photochemical multiexciton process can be exploited for initiating polymer network formation within 3D printed hydrogel composites. Low energy light can penetrate into visibly opaque hydrogels laden with TiO_2 particles, and TTA-UC chromophores activated the photoredox initiators to induce the formation of a covalent polymer network. While complementary systems that respond to visible light have emerged for initiating radical chemistries[17,62,63], our study shows that simply modifying the mechanism to activate conventional photoinitiation systems can be a powerful

tool to chemically modify objects that block high energy photons. F127-BUM hydrogels retained their printability despite the addition of the TTA-UC components and TiO_2 particles. Multi-material DIW 3DP with hydrogel composites afforded homogeneously cured constructs with mechanically enhanced properties. The fabrication of these, and other hydrogel composites, via TTA-UC will have future utility as inks for DIW 3DP to produce complex multi-material objects with low optical transparency for use in tissue engineering and soft robotics.

Supporting Information

Supporting Information is available from the Wiley Online Library or from the author.

Author Contributions

J.W. and S.W. contributed equally to this project. J.W., R.M., A.N., L.M.C. conceived the project and designed the experiments. R.M. formulated the TTA-UC system. A.N. and L.M.C. oversaw the project. R.M. and S.W. prepared the TTA-UC solutions. J.W. synthesized F127-BUM and prepared the hydrogels and composites. E.K.H. collected SAXS data. J.W. and N.A.B. performed the rheometric experiments. N.S. and J.W. designed and printed the structures. J.W. and S.W. collected data for gel fraction and tensile experiments. X.G. and S.W. collected the TEM data. J.W. and G. A.-Y. collected SEM data. J.W. and S.W. wrote the manuscript, with contributions from all authors. All authors have given approval to the final version of the manuscript.

Acknowledgements

This research is financially supported by the Center for the Chemistry of Molecularly Optimized Networks (MONET), a National Science Foundation (NSF) Center for Chemical Innovation (CHE-2116298). This research used resources of the Advanced Photon Source, a U.S. Department of Energy (DOE) Office of Science User Facility, operated for the DOE Office of Science by Argonne National Laboratory under Contract No. DE-AC02-06CH11357 (E.K.H and L.D.P. acknowledge). E.K.H. and L.D.P acknowledge support from NSF Emerging Frontiers in Research and Innovation (EFRI) program (2029249). N.S. is grateful to the University of the Basque Country (UPV/EHU) and the Margarita Salas fellowship for the requalification of the Spanish University system for 2021-2023, financed by the European Union-Next Generation EU.

Conflicts of Interest

The authors declare no conflict of interest.

Received: ((will be filled in by the editorial staff))
Revised: ((will be filled in by the editorial staff))
Published online: ((will be filled in by the editorial staff))

References

[1] Y. Zheng, W. Zhang, D. M. Baca Lopez, R. Ahmad, *Polymers* **2021**, *13*, 1957

[2] L. R. Lopes, A. F. Silva, O. S. Carneiro, *Addit. Manuf.* **2018**, *23*, 45.

[3] A. J. Boydston, B. Cao, A. Nelson, R. J. Ono, J. J. Schwartz, C. J. Thrasher, *J. Mater. Chem. A* **2018**, *6*, 20621.

[4] R. L. Truby, J. A. Lewis, *Nature* **2016**, *540*, 371.

[5] M. R. Hartings, Z. Ahmed, *Nat. Rev. Chem.* **2019**, *3*, 305.

[6] M. Layani, X. Wang, S. Magdassi, *Adv. Mater.* **2018**, *30*, 1706344.

[7] J. Zhu, R. E. Marchant, *Expert Rev. Med. Devices*, 2011, **8**, 607–626.

[8] L. J. Tan, W. Zhu, K. Zhou, *Adv. Funct. Mater.* **2020**, *30*, 2003062.

[9] Y. Bao, N. Paunović, and J.-C. Leroux, *Adv. Funct. Mater.* **2022**, *32*, 2109864

[10] Q. Ge, Z. Chen, J. Cheng, B. Zhang, Y. F. Zhang, H. Li, X. He, C. Yuan, J. Liu, S. Magdassi, S. Qu, *Sci. Adv.* **2021**, *7*, eaba4261.

[11] B. A. Frost , B. P. Sutliff , P. Thayer , M. J. Bortner, E. J. Foster, *Front. Bioeng. Biotechnol.* **2019**, *7*, 280.

[12] C. B. Highley, C. B. Rodell, J. A. Burdick, *Adv. Mater.* **2015**, *27*, 5075.

[13] Y. Fuchs, O. Soppera and K. Haupt, *Anal. Chim. Acta*, 2012, **717**, 7– 20.

[14] M. L. Gómez, R. J. J. Williams, H. A. Montejano and C. M. Previtali, *EXPRESS Polym. Lett.*, 2012, **6**, 189–197.

[15] Z. Qi, J. Xu, Z. Wang, J. Nie and G. Ma, *Int. J. Biol. Macromol.*, 2013, **53**, 144– 149.

[16] C. Ash, M. Dubec, K. Donne and T. Bashford, *Lasers Med. Sci.*, 2017, **32**, 1909–1918.

[17] D. Ahn, L. M. Stevens, K. Zhou, Z. A. Page, *Adv. Mater.* **2021**, *33*, 2104906.

[18] N. Awwad, A. T. Bui, E. O. Danilov, F. N. Castellano, *Chem* **2020**, *6*, 3071.

[19] J. Zhao, S. Ji, H. Guo, *RSC Adv.* **2011**, *1*, 937.

[20] S. K. Saha, D. Wang, V. H. Nguyen, Y. Chang, J. S. Oakdale, S. Chen, *Science* **2019**, *366*, 105.

[21] J. Xing, M. Zheng, X. Duan, *Chem. Soc. Rev.* **2015**, *44*, 5031.

[22] S. Maruo, O. Nakamura, S. Kawata, *Opt. Lett.* **1997**, *22*, 132.

[23] J. Song, C. Michas, C. H. Chen, A. E. White, M. W. Grinstaff, *Adv. Healthcare Mater.* **2020**, *9*, 1901217.

[24] K. Jung, N. Corrigan, M. Ciftci, J. Xu, S. E. Seo, C. J. Hawker, C. Boyer, *Adv. Mater.* **2020**, *32*, 1903850.

[25] J. Zhu, Q. Zhang, T. Yang, Y. Liu, R. Liu, *Nat. Commun.* ***2020***, *11*, 3462.

[26] G. S. Yi, G. M. Chow, *Adv. Funct. Mater.* **2006**, *16*, 2324.

[27] P. Bharmoria, H. Bildirir, K. Moth-Poulsen, *Chem. Soc. Rev.* **2020**, *49*, 6529.

[28] J. Zhou, Q. Liu, W. Feng, Y. Sun, F. Li, *Chem. Rev.* **2015**, *115*, 395.

[29] B. D. Ravetz, A. B. Pun, E. M. Churchill, D. N. Congreve, T. Rovis, L. M. Campos, *Nature* **2019**, *565*, 343.

[30] S. N. Sanders, T. H. Schloemer, M. K. Gangishetty, D. Anderson, M. Seitz, A. O. Gallegos, R. C. Stokes, D. N. Congreve, *Nature* **2022**, *604*, 474.

[31] S. C. Millik , A. M. Dostie, D. G. Karis, P. T. Smith, M. McKenna, N. Chan, C. D. Curtis, E. Nance, A. B. Theberge, A. Nelson, *Biofabrication* **2019**, *11*, 045009.

[32] J. Texter, R. Schwarz, *Polymer Preprints* **2005**, *46*, 1238.

[33] M. Shaikhullina, A. Khaliullina, R. Gimatdinov, A. Butakov, V. Chernov, A. Filippov, *J. Mol. Liq.* **2020**, *306*, 112898.

[34] C.-J. Wu, A. K. Gaharwar, B. K. Chan, G. Schmidt, *Macromolecules* **2011**, *44*, 8215.

[35] M. D. Biase, P. de Leonardis, V. Castelletto, I. W. Hamley, B. Derby, N. Tirelli, *Soft Matter* **2011**, *7*, 4928

[36] R. Meir, T. Hirschhorn, S. Kim, K. J. Fallon, E. M. Churchill, D. Wu, H. W. Yang, B. R. Stockwell, L. M. Campos, *Adv. Funct. Mater.* **2021**, *31*, 2010907.

[37] N. Nishimura, V. Gray, J. R. Allardice, Z. Zhang, A. Pershin, D. Beljonne, A. Rao, *ACS Materials Lett.* **2019**, *1*, 660.

[38] Q. Liu, M. Xu, T. Yang, B. Tian, X. Zhang, F. Li, *ACS Appl. Mater. Interfaces* **2018**, *10*, 12, 9883.

[39] C. S. Bahney, T. J. Lujan, C.W. Hsu, M. Bottlang, J. L. West, B. Johnstone, *Eur Cell Mater.* **2011**, *22*, 43.

[40] S. Sharifi, H. Sharifi, A. Akbari, J. Chodosh, *Sci. Rep.* **2021**, *11*, 23276.

[41] N. K. Pandit, J. Kisaka, *Int. J. Pharm.* **1996**, *145*, 129.

[42] M. Dai, Y. Tian, J. Fan, J. Ren, Y. Liu, M.D. M. Rahman, X. Ren, H. Ma, *BioRes.* **2019**, *14*, 7977.

[43] R. Xu, J. Tian, Y. Guan, Y. Zhang, *Macromolecules* **2019**, *52*, 365.

[44] M. A. Abou-Shamat, J. Calvo-Castro, J. L. Stair, M. T. Cook, *Macromol. Chem. Phys.* **2019**, *220*, 1900173.

[45] R. K. Prud'homme, G. Wu, D. K. Schneider, *Langmuir* **1996**, *12*, 4651.

[46] K. Mortensen, W. Batsberg, S. Hvidt, *Macromolecules* **2008**, *41*, 1720.

[47] K. Rezwana, Q.Z. Chena, J.J. Blakera, A. R. Boccaccini, *Biomaterials* **2006**, *27*, 3413.

[48] D. Jiang, F. Ning, Y. Wang, *J. Mater. Process. Technol.* **2021**, *289*, 116952.

[49] Q. Ma, Y. Zhang, V. Launay, M. L. Dot, S. Liu and J. Lalevée, *Eur. Polym. J.*, 2022, **165**, 111011.

[50] T. Zhao, X. Li, R. Yu, Y. Zhang, X. Yang, X. Zhao, L. Wang, W. Huang, *Macromol. Chem. Phys.* **2018**, *219*, 1700530.

[51] N. D. Dolinski, E. B. Callaway, C. S. Sample, L. F. Gockowski, R. Chavez, Z. A. Page, F. Eisenreich, S. Hecht, M. T. Valentine, F. W. Zok, C. J. Hawker, *ACS Appl. Mater. Interfaces* **2021**, *13*, 22065.

[52] M. A. Skylar-Scott, J. Mueller, C. W. Visser, J. A. Lewis, *Nature* **2019**, *575*, 330.

[53] K. Chen, L. Zhang, X. Kuang V. Li, M. Lei, G. Kang, Z. L. Wang, H. J. Qi, *Adv. Funct. Mater.* **2019**, *29*, 1903568.

[54] Dimitri Kokkinis, Manuel Schaffner, Andre´ R. Studart, *Nat. Commun.* **2015**, *6*, 8643.

[55] V. G. Rocha, E. Saiz, L. S. Tirichenko, E. García-Tuñón, *J. Mater. Chem. A* **2020**, *8*, 15646.

[56] J. Wong, A. Basu, M. Wende, N. Boechler and A. Nelson, *ACS Appl. Polym. Mater.*, 2020, **7**, 2504–2508.

[57] K. Chen, X. Kuang, V. Li, G. Kang, H. J. Qi, *Soft Matter* **2018**, *14*, 1879.

[58] U. Jammalamadaka, K. Tappa, *J. Funct. Biomater.* **2018**, 9, 22.

[59] R. C. Advincula, J. R. C. Dizon, E. B. Caldona, R. A. Viers, F. D. C. Siacor, R. D. Maalihan, A. H. Espera Jr., *MRS Communications* **2021**, *11*, 539.

[60] W. Zhu, X. Ma, M. Gou, D. Mei, K. Zhang, S. Chen, *Curr. Opin. Biotechnol.* **2016**, *40*, 103.

[61] J. V. Karpiak, Y. Ner, A. Almutairi, *Adv. Mater.* **2012**, *24*, 1466.

[62] D. Ahn, L. M. Stevens, K. Zhou, Z. A. Page, *ACS Cent. Sci.* **2020**, *6*, 1555.

[63] Z. Wu, K. Jung, C. Boyer, *Angew. Chem. Int. Ed.* **2020**, *59*, 2013.

Direct-ink-write printing and photocuring of opaque hydrogel composites is enabled by multiexciton triplet-triplet annihilation upconversion. Low energy red light is used for better penetration into opaque hydrogels and the upconverted blue light induces the free radical photopolymerization process. This method allows conventional photoinitiation systems to modify objects that block high energy photons.

Jitkanya Wong †, Shixuan Wei †, Rinat Meir, Naroa Sadaba, Nathan A. Ballinger, Elizabeth K. Harmon, Xin Gao, Gokce Altin-Yavuzarslan, Lilo D. Pozzo, Luis M. Campos*, Alshakim Nelson*

Triplet Fusion Upconversion for Photocuring 3D Printed Particle-Reinforced Composite Networks

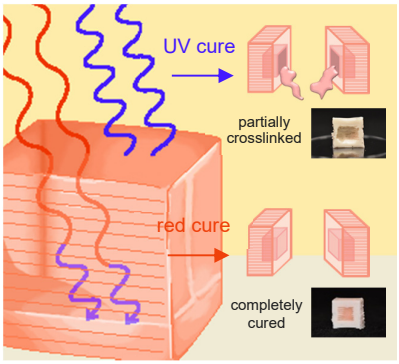

Supporting Information

Triplet Fusion Upconversion for Photocuring 3D Printed Particle-Reinforced Composite Networks

Jitkanya Wong†, Shixuan Wei†, Rinat Meir, Naroa Sadaba, Nathan A. Ballinger, Elizabeth K. Harmon, Xin Gao, Gokce Altin-Yavuzarslan, Lilo D. Pozzo, Luis M. Campos, Alshakim Nelson**

Experimental Section

Materials: Pluronics® F127 (BioReagent), triethanolamine (98%), Eosin Y (99%), Titanium(IV) oxide (325 mesh), >99%) and $CDCl_3$ (D, 99.8% + 1% V/V TMS) were purchased from MilliporeSigma. Titanium(IV) oxide (NanoArc, 32 nm APS powder, 99.9%) was purchased from Alfa Aesar. 2-isocyanatoethyl methacrylate (>98%), dibutyltin dilaurate (>95%), and 2-hydroxy-2-methylpropiophenone (>96%) were purchased from TCI America. PdTPTBP was purchased from Santa Cruz Biotechnology, Inc. TIPS-anthracene was synthesized according to the reported procedure.[1] Diethyl ether, acetone, and tetrahydrofuran (HPLC grade) were purchased from Fisher Scientific. All reagents were used as received. Anhydrous methylene chloride was obtained by purification over alumina column on a Pure Process Technology purification system. Soybean oil was purchased from Alfa Aesar.

TTA-UC Solution Preparation: PdTPTBP (2.5 mg) was dissolved in tetrahydrofuran (1.00 mL) as a stock solution. To the freshly prepared stock solution (100 µL) was added TIPS-anthracene (14.0 mg). Tetrahydrofuran (900 µL) was added to completely dissolve the TIPS-anthracene followed by the addition of soybean oil (1.00 mL). The control solution was made in the same way without addition of the TIPS-anthracene.

F127-BUM Synthesis: Glassware was oven-dried at 125 °C for at least 16 h and F127 polymer (60 g, 4.8 mmol) was dried under vacuum (~ 2 Pa) for at least 16 h at room temperature in a round-bottom flask. Anhydrous dichloromethane (550 mL) was added to the flask under N_2 atmosphere. The mixture was stirred at 30 °C, and after the polymer has dissolved, dibutyltin dilaurate (12 drops) was added using a glass Pasteur pipette. The 2-isocyanatoethyl methacrylate (3.5 mL, 24.8 mmol) was diluted in anhydrous dichloromethane (50 mL) and added to the reaction mixture at a rate of approximately 1 drop/s. The reaction was left to stir under N_2 at 30 °C. After 2 d, the reaction was concentrated at 30 °C using a rotary evaporator. The polymer was precipitated by slowly pouring the concentrate into diethyl ether (1.8 L) in a large beaker. The precipitate mixture was stirred for an additional 30 min before turning off stirring to let the precipitate settle for 2 h. Diethyl ether was decanted off and the precipitate was then washed twice by adding diethyl ether (1 L), stirring for 15 min, and letting settle for 1 h. After the second washing, ether was decanted and the remaining residual amount was allowed to evaporate by agitating with a spatula under an N_2 flow. The resultant F127-BUM powder (56 g, 93.3% yield) was dried fully overnight at room temperature under vacuum (~ 2 Pa) and stored in the dark at 4 °C until further use.

Preparation of Hydrogels: The standard UV-cure hydrogels (5 g scale) were prepared by combining F127-BUM (1.5 g), TiO_2 (5(0.0x) g; x = percent TiO_2), deionized water (3.5 − 5(0.0x) g), and 2-hydroxy-2-methylpropiophenone (5 μL). The upconversion hydrogels were prepared by combining F127-BUM, TiO_2, and deionized water. Triethanolamine (13.56 wt% solu. in PBS), Eosin Y (0.647 wt% solu. in PBS), and upconversion solution were then added via volumetric pipette, vortexed until mostly homogenous, and stored at 4 °C overnight to let F127-BUM dissolve. The amounts of each components used to make the upconversion hydrogels are summarized in **Table S1**. With the exception of tensile test and the gel fraction experiment for TTA-UC hydrogels, where both 32 nm and 325 mesh TiO_2 particles were used, all other experiments used the 325 mesh TiO_2 particles.

Table S1. Formulations for TTA-UC Hydrogel/TiO_2 (325 mesh) Composite (5g scale)

% TiO_2	F127-BUM [g]	TiO_2 [g]	DI H_2O [g]	TEA solu. [μL]	Eosin Y solu. [μL]	UC solu. [μL]
0	1.5	0	3.393	37	50	20
1	1.5	0.05	3.343	37	50	20
2	1.5	0.10	3.293	37	50	20
5	1.5	0.25	3.143	37	50	20

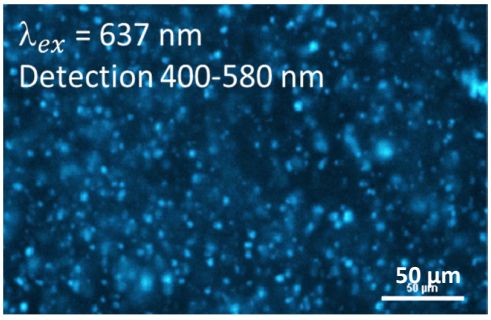

Figure S1. TTA-UC mixture containing sensitizer, annihilator, tetrahydrofuran, water, and soybean oil. Emission from 400-580 nm was detected. Image is pseudocolored blue for clarity.

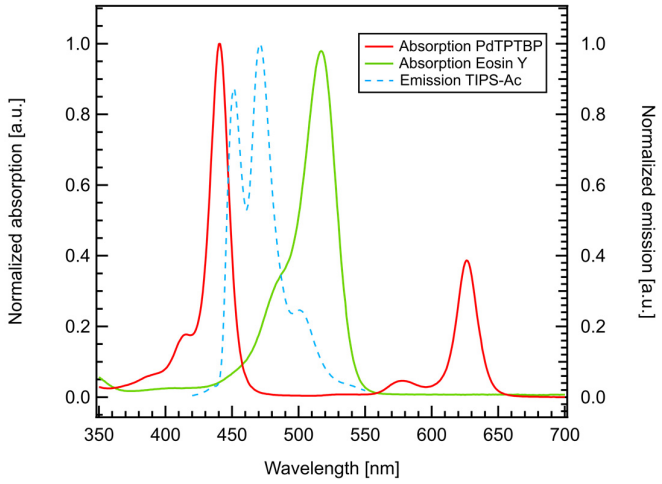

Figure S2. Absorption spectra of PdTPTBP in dilute THF and Eosin Y in dilute PBS and emission spectrum of TIPS-anthracene in dilute THF.

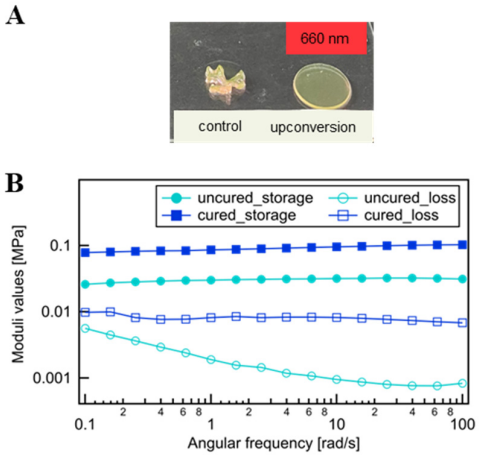

Figure S3. Characterization of materials after photocuring. Red light curing of the TTA-UC and control gels (A), showing all components of TTA-UC system was required for photocuring with red light, and a frequency sweep rheometric experiment (B) to show the three-fold, irreversible increase of storage moduli after photocuring.

Light source for photocuring: For all UV curing, samples were placed in a box with 2 365 nm Sunlite A19 UV Lamp bulbs, with measured intensity of 8.0 mW/cm^2. For the blue light and green light gel fraction control experiment, H150-Blue and PR160L-525 Kessil lamps were used. The intensities measured were 12.6 mW/cm^2 and 9.7 mW/cm^2 (**Figure S4**A, B). For all red light curing, samples were placed in a box with 660 nm Mrhua LED Grow light (UFO) (**Figure S4**C), with measured intensity of 5.24 mW/cm^2.

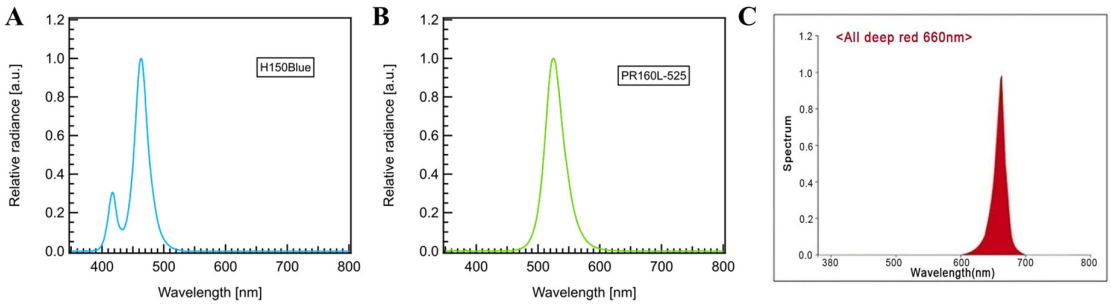

Figure S4. Emission spectra of the light sources. A) blue light (H150Blue), and B) green light (PR160L-525). C) red light.

SAXS: Small-angle X-ray scattering (SAXS) was performed on beamline 12-ID-C at the Advanced Photon Source at Argonne National Laboratory over a Q-range of 0.01 to 1.3 $Å^{-1}$ in a pinhole configuration**.** The instrument used an X-ray source of 20 keV, corresponding to a wavelength of 0.62 Å, a beam size of 0.4 mm x 0.15 mm and a flux density of approximately 2 X 10^{12} photons/s/mm^2. Samples were loaded and cured in place in a custom aluminum 48 well plate, sealed between two Kapton windows.[2] SAXS data were collected at room temperature and with exposure times of 1 second each. Scattering profiles were radially integrated on-site using locally authored MATLAB software and were normalized using Kapton background subtraction.

SAXS data (**Figure S5**) suggested there was no significant increase in the q-value, which represents the average intermicellar distance, in the presence of the TTA-UC additives. Thus, the presence of emulsion droplets (**Figure S1**) from the TTA-UC solution does not alter the F127 micelle size and packing. The ratios of normalized Q-values amongst the peaks for both samples suggest the BCC packing of micelles.

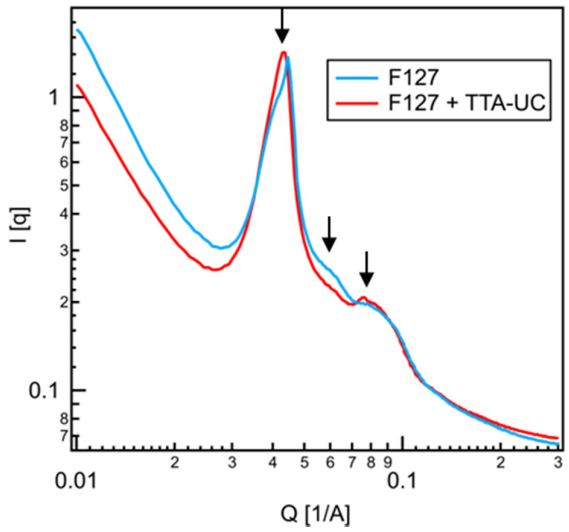

Figure S5. SAXS data for F127 hydrogel with and without TTA-UC additives.

Rheology: Rheometric characterization was performed on a TA Instruments DHR-2 equipped with an Advanced Peltier Plate system. All experiments were performed using the 8 mm flat stainless steel upper plate. The sample was cooled to 0 °C, then loaded by pouring the gel onto the bottom plate. The sample is then trimmed after the upper plate was lowered to the trim gap at 600 μm. The final geometry gap was then set to 500 μm, and pre-shear was applied at 5 °C for 10 s before additional sample conditioning at 25 °C for 8 min. The strain sweep experiment (**Figure S6**A) was performed to measure the storage and loss moduli over 0.01 to 100% strain (1 Hz). The storage moduli at low strains (< 1%) were 30-40 kPa, suggesting firm gels that can support the load from subsequent layers in a multi-layered construct. Upon increasing applied strain, the materials exhibited a yielding behavior where the storage modulus decreased rapidly the loss modulus eventually exceeded the storage modulus. This gel-to-sol transition allows the hydrogels to flow out of the nozzle during the printing process. The cyclic shear strain experiment (**Figure S6**B) was performed at 25 °C using alternating strains of 1% for 5 min and 100% for 3 min (1 Hz) showed that the changes in the moduli are reversible and instantaneous. The results show that the hydrogel can be extruded from a nozzle with an immediate response to applied force, and quickly recovers its gel state upon exiting the nozzle. The frequency sweep experiment was performed to measure the storage and loss moduli at 1% strain over frequency range of 0.1 to 100.0 rad/s (equivalent to 0.0159-15.9 Hz). For the frequency sweep, the uncured material is trimmed at 1050 μm trim gap and the final gap is 1000 μm. For the frequency sweep on cured upconversion material, the gel was sandwiched between 2 microscope glass slides (using additional glass slides as spacers), and cured until 660 nm light for 25 minutes, and an 8 mm Royaltek biopsy punch was used to obtain the final sample. The sample is then placed on the geometry, which was lowered to a gap of 1000 μm (measured axial force = 1.7 N) for the data collection. This experiment was done with samples of maximum particle loading of 15 wt% TiO_2 (325 mesh, **Figure S7**), as any higher filler loading resulted in visible settling.

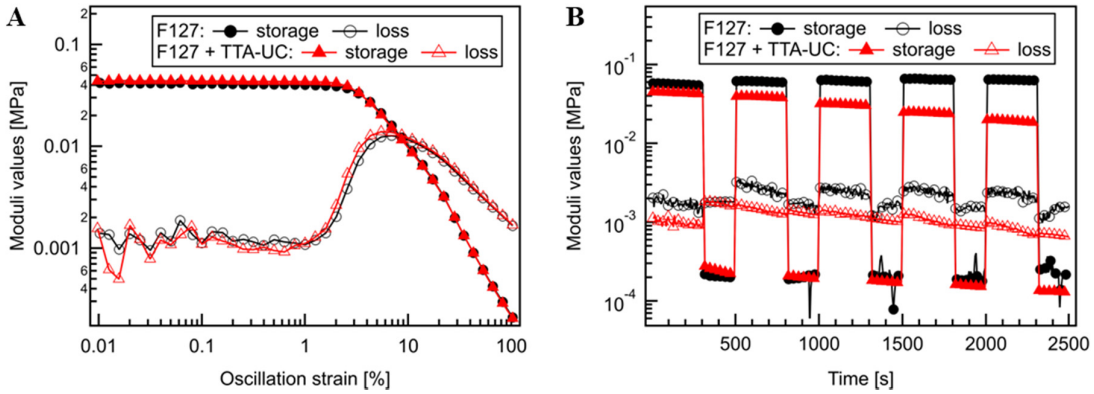

Figure S6. Rheometric characterization includes A) strain sweep and B) cyclic strain experiments.

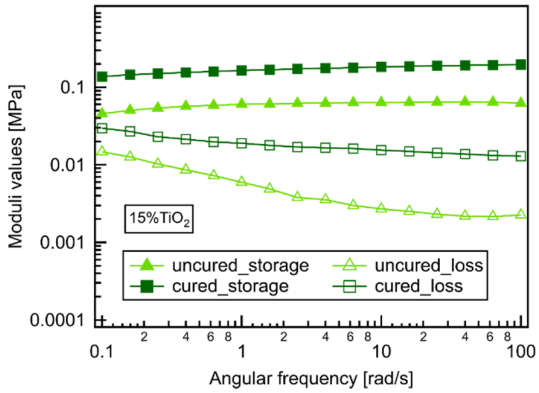

Figure S7. Frequency sweep rheometric experient to show the irreversible increase of storage moduli for the cured material at the maximum amount of TiO_2 (325 mesh) loading tested at 15 wt%.

Gel Fraction: Cooled hydrogels are poured into a Sylgard mold for cylindrical samples (radius 10 mm, 5 mm height). Excess material was removed with a razor, and a large glass slide was placed over the top of the mold. The samples are then irradiated with 660 nm light for 25 min, and the entire setup was flipped and irradiated for an additional 5 min. The original masses are recorded, cut in halves and placed in tared scintillation vials with 10 mL acetone. The samples are then left for a specified amount of time, as shown in **Figures 2**B-E, and acetone was decanted off and the vials are placed into vacuum oven for at least 24 h before mass of each

sample is collected. The gel fractions are calculated by taking the ratio between the collected mass and the calculated dry original mass (original mass multiplied by percent of expected F127-BUM and TiO_2 in each formulation).

As a control experiment, we have also collected gel fraction data for samples cured using blue light (447.5 nm) to observe curing using with light in the same emission range as TIPS-anthracene. Similarly, the transparent samples showed similar gel fractions compared to the red light cured samples, while the samples containing TiO_2 showed significantly lower gel fractions.

Table S2. Formulations for Irgacure 2959 Hydrogel/TiO_2 (325 mesh) Composite (5g scale)

% TiO_2	F127-BUM [g]	TiO_2 [g]	DI H_2O [g]	Irgacure 2959 [μL]
0	1.5	0	3.495	5
1	1.5	0.05	3.445	5
2	1.5	0.10	3.395	5
5	1.5	0.25	3.245	5

Table S3. Formulations for Eosin Y/TEA Hydrogel/ TiO_2 (325 mesh) Composite (5g scale)

% TiO_2	F127-BUM [g]	TiO_2 [g]	DI H_2O [g]	TEA solu. [μL]	Eosin Y solu. [μL]	THF/soybean oil = 1:1 [μL]
0	1.5	0	3.393	37	50	20
1	1.5	0.05	3.343	37	50	20
2	1.5	0.10	3.293	37	50	20
5	1.5	0.25	3.143	37	50	20

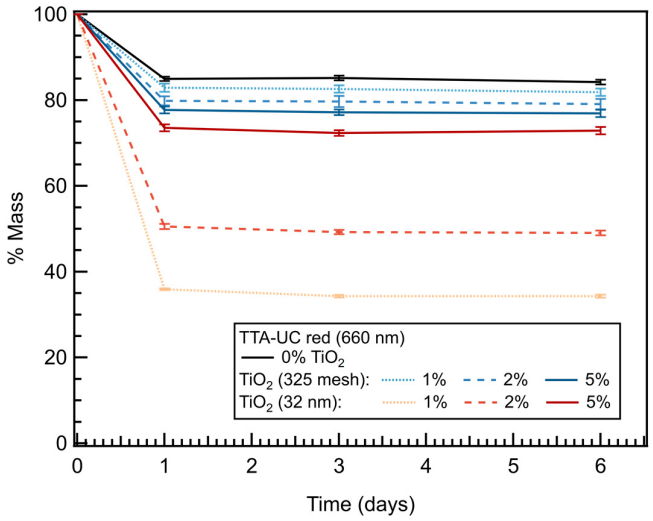

Figure S8. Comparison of tracked mass loss during gel fraction experiments for TTA-UC samples with TiO_2 (32 nm) and TiO_2 (325 mesh) cured via red light.

Tensile Tests: TestResources Universal Test System 1.1 kN electromechanical actuator single column load frame with a 44 N high accuracy S10 type load cell was used to evaluate the mechanical properties of the cured hydrogels. For dimensions of all dogbones, ASTM D638 type V specimen specifications were used. The dogbones were prepared by pouring the cooled hydrogel into a Teflon dogbone. Excess material was scraped off by a razor and a microscope glass slide was placed on top. The gel was then exposed to 660 nm light for 25 min, then removed from the mold, flipped and cured for an additional 5 min. The sample was then attached to the vice grips with diamond grit jaw and subjected to increasing strain at a constant rate of 10 mm/min until mechanical failure.

To probe the effect of particle size, we did measurements on hydrogels filled with 32 nm or 325 mesh TiO_2 particles. With increasing amount of TiO_2 (325 mesh), the Young's moduli increased and the maximum strain decreased (**Figure 3**). For the addition of TiO_2 (32 nm, **Figure S10** and **Figure S11**), the particles initially have a plasticizing effect at low concentrations, reducing the Young's moduli and increasing the maximum strain, but ultimately stiffened the material as we increased the amount. The ability to either stiffen or soften the material with different types, size, and concentration of particles[3–5], and the limit to filler

concentration that contributes to the change in mechanical properties aligned with other observations in literature.[6-8] While the increase in filler amount from 2 to 5 wt% of the TiO_2 (32 nm) particles seemed to have a significant increase in stiffness, there was no significant difference for the TiO_2 (325 mesh) particles. This observation was attributed to the difficulty in dispersing larger particles in the hydrogel, as settling can occur and prevent the filler from effectively tuning the mechanical properties. While this study was only limited to 2 types of fillers, we were able to obtain a wide range of Young's modulus ranging from 27.98±0.46 to 80.2±5.8 kPa, falling into the same range of many soft biological tissues (vocal ligament 33.1 kPa[9], cardiac tissue 5-50 kPa[10], lens 54 kPa[11], glandular breast tissue 48-66 kPa[12], skin 50-150 kPa[13]). Additionally, our values were in similar range to many reported soft hydrogels systems developed for biological tissue mimics.[14–16] In future studies, varying the polymer composition, type and particle size of fillers can also further expand the range of mechanical properties.

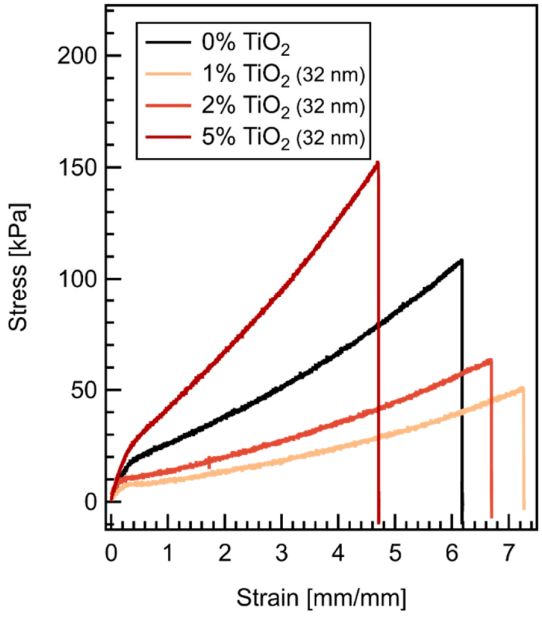

Figure S9. Tensile stress-strain curves for hydrogel dogbone (ASTM D638 type V) samples with varying amounts of TiO_2 (32 nm), cured by TTA-UC with 660 nm light.

Table S4. Calculated Young's modulus and maximum strain from tensile test in **Figure 3** & **Figure S9** and comparison of TiO_2 particles (325 mesh) versus TiO_2 nanoparticle (32 nm).

	0% TiO_2 (325 mesh)	1% TiO_2 (325 mesh)	2% TiO_2 (325 mesh)	5% TiO_2 (325 mesh)	1% TiO_2 (32 nm)	2% TiO_2 (32 nm)	5% TiO_2 (32 nm)
Young's Modulus [kPa]	53.63±0.99	51.2±4.9	73.2±1.2	79.1±4.1	27.98±0.46	36.8±2.0	80.2±5.8
Maximum Strain [mm/mm]	5.70±0.63	4.51±0.36	4.00±1.4	5.50±1.2	6.51±0.53	5.65±0.83	3.69±1.2

Transmission Electron Microscopy: TiO_2 particles were dispersed in Millipore water and dried on a TEM grid in a desiccator for 2 hours. TEM image was acquired by FEI Talos F200X S-TEM operating at 200kV.

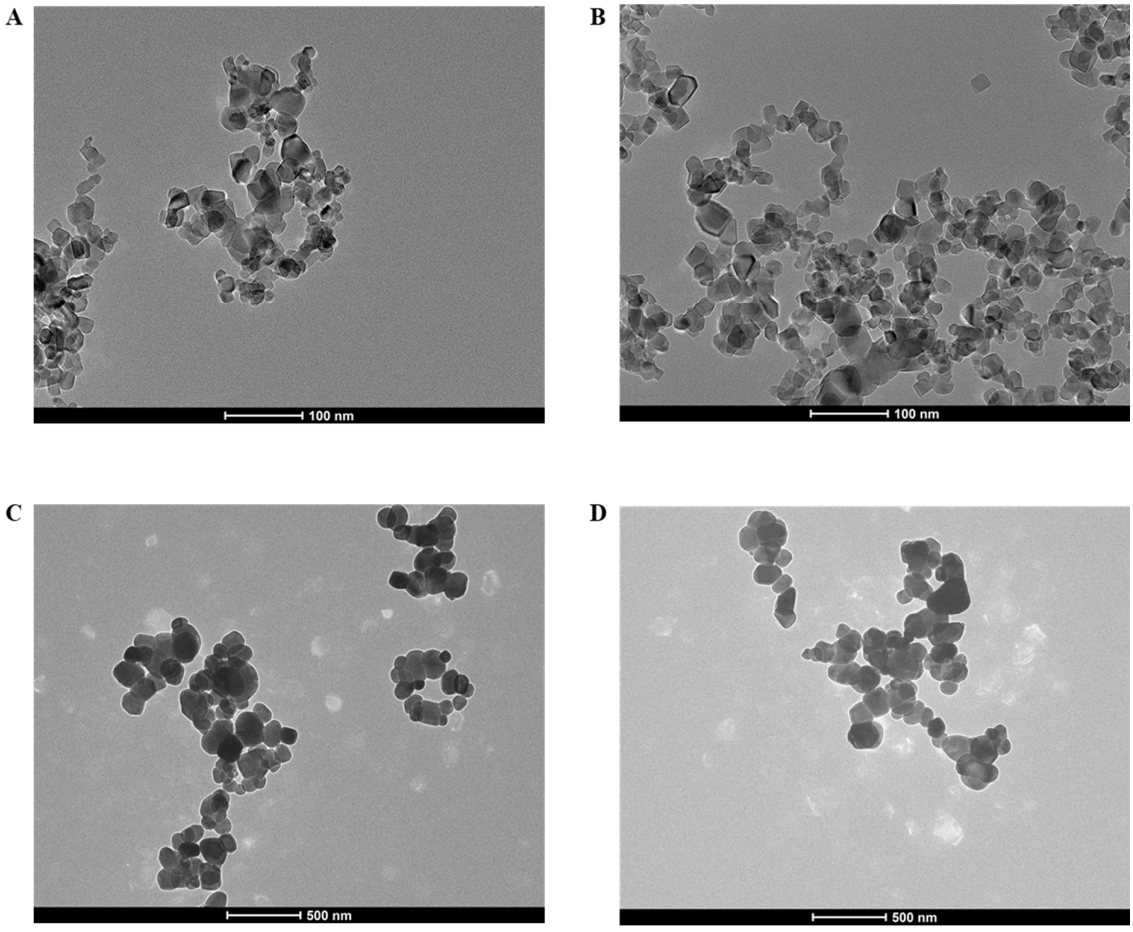

Figure S10. TEM images of the TiO_2 particles of different sizes. A) and B) 32 nm. C) and D) 325 mesh.

Scanning Electron Microscope Images: For SEM image collection, the TTA-UC hydrogel samples containing either 32 nm or 325 mesh TiO_2 particles, cured by red light, were placed in a vacuum oven overnight to remove all water. The samples were then scored with a razor, dipped in liquid nitrogen, cracked with a spatula to introduce a new surface, and coated with Pt (4 nm) by Leica EM ACE600. SEM images were obtained using the Sirion XL30 scanning electron microscope, operated under high vacuum, with an acceleration voltage of 20 kV, and spot size of 3.

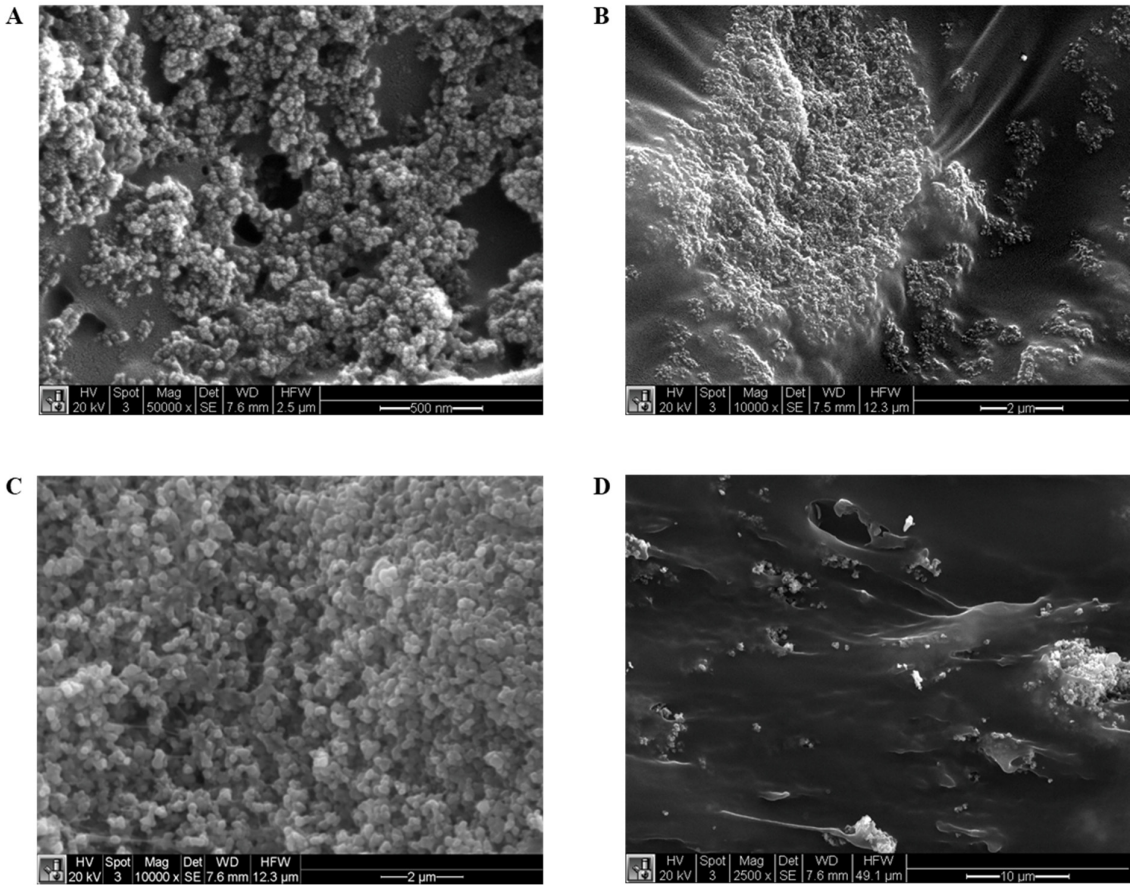

Figure S11. SEM images of vacuum-dried TTA-UC hydrogels filled with TiO_2 of different sizes, cured by red light. A) and B) hydrogels filled with TiO_2 (32 nm). C) and D) hydrogels filled with TiO_2 (325 mesh). All samples showed polydisperse and aggregated particles that ranged from sub-micron to a few of microns.

DIW Printing of Hydrogel Composites: Direct Ink Write 3D printing was performed on a HyRel Engine SR extrusion printer with SDS-5 syringer dispenser. The G-codes were written through a text editor. All printing was performed using F127-BUM upconversion system inks

with an extrusion rate of 81 pulse/μL. The structures were printed with a layer height of 0.6 mm, with print speeds at 300 mm/min. After printing was completed, the printed structures are placed into a sealed petri dish and purged with argon before curing with red light for 25 minutes, followed by direct light curing with the petri dish lid off for another 10 minutes. For the printed pristine and composite dogbones in **Figure 4**H, EN ISO 527-2:1996 type 5B specimen specifications were used.

References

[1] R. Meir, T. Hirschhorn, S. Kim, K. J. Fallon, E. M. Churchill, D. Wu, H. W. Yang, B. R. Stockwell, L. M. Campos, *Adv. Funct. Mater.* **2021**, *31*, 2010907

[2] L. D. Pozzo. 'SAXS-USAXS Liquids 48 well plate holder', can be found under https://github.com/pozzo-research-group/Automation-Hardware/tree/master/Cartridge%20Sample%20Holder%20for%20SAS%20Experiments/SAXS-USAXS%20Liquids%2048%20well%20plate%20holder, **2022**.

[3] A. Gantar, L. P. da Silva, J. M. Oliveira, A. P. Marques, V. M. Correlo, S. Novak, R. L. Reis, *Mater. Sci. Eng.* **2014**, *43*, 27.

[4] C. Czichya, J. Spangenberg, S. Günthera, M. Gelinsky, S. Odenbach, *J. Magn. Magn. Mater.* **2020**, *501*, 166395.

[5] Y. Yu, H. Yuk, G. A. Parada, Y. Wu, X. Liu, C. S. Nabzdyk, K. Youcef-Toumi, J. Zang, X. Zhao, *Adv. Mater.* **2019**, *31*, 1807101.

[6] J. Song, C. Michas, C. H. Chen, A. E. White, M. W. Grinstaff, *Adv. Healthcare Mater.* **2020**, *9*, 1901217.

[7] S. Utech, A. R. Boccaccini, *J. Mater. Sci.* **2016**, *51*, 271.

[8] T. S. Jang, H. D. Jung, H. M. Pan, W. T. Han, S. Chen, J. Song, *Int. J. Bioprint.* **2018**, *4*, 126.

[9] Y. B. Min, I. R. Titze, F. Alipour-Haghighi, *Ann. Otol. Rhinol. Laryngol.* **1995**, *104*, 563.

[10] I. J. Domian, H. Yu, N. Mittal, *Adv. Healthcare Mater.* **2017**, *6*, 1600768.

[11] K. R. Heys, S. L. Cram, R. J. W. Truscott, *Mol. Vis.* **2004**, *10*, 956.

[12] G. Singh, A. Chanda, *Biomed. Mater.* **2021**, *16*, 062004.

[13] C. F. Guimarães, L. Gasperini, A. P. Marques, R. L. Reis. *Nat. Rev.* **2020**, *5*, 351.

[14] V. R. Feig, H. Tran, M. Lee, Z. Bao, *Nat. Commun.* 2018, *9*, 2740.

[15] R. Chen, X. Xu, D. Yu, C. Xiao, M. Liu, J. Huang, T. Mao, C. Zheng, Z. Wang, X. Wu, *J. Mater. Chem. C* **2018**, *6*, 11193.

[16] G. Tronci, A. T. Neffe, B. F. Pierce, A. Lendlein, *J. Mater. Chem.* **2010**, *20*, 8875.